Catalysis Science & Technology

ROYAL SOCIETY OF CHEMISTRY

PAPER

View Article Online
View Journal | View Issue

Cite this: *Catal. Sci. Technol.*, 2021, **11**, 1358

Coupling conversion of methane with carbon monoxide *via* carbonylation over Zn/HZSM-5 catalysts†

Fuli Wen,[abc] Jin Zhang,[abc] Zhiyang Chen,[abc] Ziqiao Zhou,[abc] Hongchao Liu,*[ab] Wenliang Zhu*[ab] and Zhongmin Liu [abc]

Received 11th October 2020,
Accepted 26th November 2020

DOI: 10.1039/d0cy01983f

rsc.li/catalysis

Efficient direct transformation of methane into value-added chemicals has great significance for long-term sustainability of fuels and chemicals, but remains a major challenge due to its high inertness. Reported here is that methane can be activated effectively *via* carbonylation with CO over Zn/HZSM-5 catalysts under mild conditions. The selectivity to aromatics alone reaches 80% among all hydrocarbon products at 823 K, whereas as high as 92% ethane selectivity is achieved at a lower temperature of 673 K. ^{13}CO isotope labelling experiments demonstrate that approximately 50% of the carbon atoms in all the products originate from carbon monoxide, whereas another half of the carbons come from methane, indicating that the precursors of hydrocarbon products are acyl compounds and/or acetic acid formed by carbonylation of methane with carbon monoxide. This provides potential for transformation of methane into value-added chemicals under mild reaction conditions.

1. Introduction

Natural gas is the cleanest fuel among all fossil fuel resources and widely used in industry and our daily life.[1] In recent years, the production of natural gas has been significantly increased due to the breakthrough of hydraulic fracturing technology, especially in the United States.[2] However, the application of natural gas is still restricted to combustion for heating systems and only about 15% of natural gas is used as chemical raw materials.[1] Considering the limitation of oil reserves and rising demands for sustainable liquid fuels and chemicals,[3] natural gas is considered to be one of the promising replacements of petroleum in the near future and, therefore, transformation of natural gas into value-added commodities by economically viable processes has attracted much attention in the fields of scientific research and industrial production.

In all routes of natural gas conversion, the process of indirect conversion of natural gas into fuels and chemicals has been commercialized with syngas (a mixture of H_2 and CO) as a platform followed by Fischer–Tropsch synthesis or methanol conversion to bulk chemicals,[4] despite its complex production process, high capital cost and energy consumption, and huge emission of carbon dioxide.[5] Due to the removal of oxygen from CO by formation of either water or CO_2 during hydrocarbon synthesis, the conversion of natural gas *via* syngas is a lower atom-economic process in comparison to the direct conversion of natural gas. The latter is possibly more environmentally friendly and economical in terms of utilization efficiency of both carbon and hydrogen atoms. Unfortunately, the activation of methane (the main component of natural gas) is a big challenge so far, attributed to the high C–H bond strength (434 kJ mol^{-1}) and extremely symmetric molecular structure of methane, which results in the highly inert properties of methane molecule.[6] In turn, severe reaction conditions are indispensably required during direct conversion of methane in order to achieve a high yield of desired products, *e.g.* the pyrolysis temperature of methane for production of aromatics and hydrogen is as high as about 1400 K.[5,7]

To activate the C–H bond of methane under mild reaction conditions, some assistants, such as oxygen,[8–10] carbon dioxide,[11] methanol[12] or hydrocarbons,[2,13–16] were introduced into reaction systems for coupling conversion of methane. In such routes, oxidative coupling of methane (OCM) for production of ethylene, discovered by Keller *et al.*[17] in 1982, is a representative example. In the past few decades, scientists have made great efforts in this field. Unfortunately, due to the strong oxidation of oxygen, over-oxidation of methane

[a] *National Engineering Laboratory for Methanol to Olefins, Dalian Institute of Chemical Physics, Chinese Academy of Sciences, Dalian 116023, China*
[b] *Dalian National Laboratory for Clean Energy, Dalian Institute of Chemical Physics, Chinese Academy of Sciences, Dalian 116023, China.*
E-mail: chliu@dicp.ac.cn, wlzhu@dicp.ac.cn
[c] *University of Chinese Academy of Sciences, Beijing 100049, China*

† Electronic supplementary information (ESI) available. See DOI: 10.1039/d0cy01983f

occurs inevitably and large amounts of water, carbon monoxide and carbon dioxide are yielded, resulting in a low efficiency of the OCM process.[18,19] In addition, the heat from the highly exothermic reaction of methane with oxygen is hazardous in a large scale.[13]

Previous studies on direct catalytic conversion of methane with CO are rather limited, and most of them were performed in a homogeneous reaction system for production of acetic acid,[20–24] which is not suitable for large-scale conversion of natural gas at high reaction temperature, and the efficiency for products remains a challenge. On the other hand, heterogeneous catalytic processes are conventional approaches for production of bulk chemicals in a large-scale and offer the potential for conversion of methane to value-added chemicals. However, there are very few studies on the conversion of methane with CO by carbonylation in a heterogeneous reaction system, especially for the production of aromatics. In 1997, Shuichi Naito *et al.*[25] evaluated several silica-supported Rh, Ru and Pd catalysts in a CH_4 + CO conversion reaction at 573–723 K, and found that the formation of benzene containing a small amount of carbon atoms originated from methane. Wang[26] and Ichikawa[27,28] reported that the presence of CO in a methane feed has a significant promotion effect on the stability and productivity of HZSM-5 catalysts, which were modified with Zn, Mo or Re, during the transformation of methane into aromatics. On the basis of *in situ* solid-state NMR spectroscopy studies, Deng[29] found that methane could be directly transformed into acetic acid with CO by carbonylation over ZnZSM-5 catalysts under mild conditions, but no aromatics were detected in their studies.

Here, we report research on the coupling conversion of methane with CO by carbonylation over Zn/HZSM-5 catalysts in a heterogeneous reactor, and found that methane can be efficiently activated and converted into hydrocarbons in the presence of CO, and in particular selectivity to aromatics could reach about 80% at 823 K. Meanwhile, at a relatively low reaction temperature of 673 K, the main products were gaseous hydrocarbons and an ethane selectivity as high as 92% was achieved. Unexpectedly, the ^{13}CO isotope labelling experiments show that approximately 50% of the carbon atoms in all the products originated from carbon monoxide, and the rest from methane. Such interesting results indicate that intermediate species (precursors) in the formation of aromatics must be acetyl compounds, which are yielded by carbonylation of methane with CO over Zn/HZSM-5.

2. Experimental

2.1 Catalyst preparation

Commercial HZSM-5 zeolite (SiO_2/Al_2O_3 = 40, NanKai University) was first tableted, crushed and sieved to 40–60 mesh, and then calcined at 550 °C for 5 h in air prior to impregnation. Zn/HZSM-5 catalyst was prepared by an incipient wetness method with aqueous solutions containing desired amounts of zinc nitrate. After impregnation and drying at 120 °C for 2 h, the sample was calcined in air at 550 °C for 4 h in muffle. The corresponding weight percentage of zinc in the prepared catalyst is approximately 5.9%, as determined by XRF. The prepared catalyst was denoted as Zn/HZSM-5.

2.2 Catalyst characterization

HZSM-5 zeolite morphology was determined by scanning electron microscopy at 2.0 kV using a Hitachi SU8020 instrument. BET surface areas and pore volumes were obtained by nitrogen sorption experiments at 77 K using a Micromeritics ASAP-2020 analyzer. The samples were degassed in a flow of nitrogen at 350 °C for 4 h prior to each measurement. The ratio of silica to alumina was achieved by XRF on a PANalytical AXIOS spectrometer. The surface morphology of the catalysts was achieved using a field-emission scanning electron microscope (FE-SEM, SU8020). Transmission electron microscopy images (TEM) were obtained on a JEM-2100F microscope. Ammonia temperature-programmed desorption (NH_3-TPD) experiments were performed using a Micromeritics AutoChem 2920 instrument. In a typical NH_3-TPD experiment, about 200 mg of catalyst sample was loaded in a quartz tube and purged at 600 °C with helium for 30 min to remove the moisture from the sample. Then, the catalyst sample was cooled to 100 °C and saturated with NH_3. After purging with He to remove physically adsorbed ammonia, the desorption experiment was conducted from 100 to 650 °C at a heating rate of 10 °C min^{-1} in a He flow.

^{13}C CP/MAS NMR solid-state NMR spectroscopy experiments were conducted as follows. ^{13}C labelled carbon monoxide was used to react with methane over Zn/HZSM-5. The working catalyst was quenched by liquid nitrogen under reaction conditions quickly, taken out from the reactor and transferred into a 4 mm NMR rotor for NMR spectroscopy in the glove box. All the solid-state NMR experiments were performed on a Bruker Avance III 600 spectrometer equipped with a 14.1 T wide-bore magnet using a 4 mm MAS probe. ^{13}C CP/MAS NMR spectra were recorded using a cross polarization sequence with a spinning rate of 12 kHz.

^{13}C isotope experiments were conducted by co-reaction of CH_4 with ^{13}CO at 773 K and 1.0 MPa. The reaction effluent was collected firstly using dichloromethane as a solvent, and the gas phase mixtures being undissolved in dichloromethane were collected by a gas sampling bag for a 60 min reaction. The obtained liquid and gas phase samples were analysed by GC-MS.

2.3 Catalytic tests

The catalyst was tested on a high-pressure fixed bed reactor (inner diameter was 10 mm), with a quartz tube (outer diameter was 8 mm) placed inside the stainless-steel tube. Typically, 0.4 g catalyst was packed into the reactor, pre-treated with He at 350 °C for 2 h and then heated to reaction temperature in 30 min. After the pre-treatment, the mixture gas with a composition of 10% methane, 80% carbon monoxide, and 10% argon was introduced to the reactor. The reaction

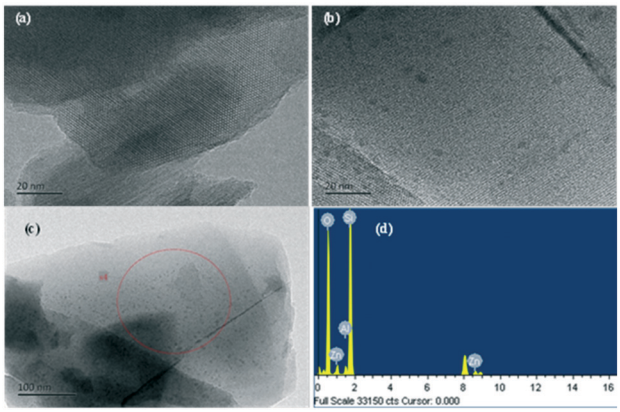

Fig. 1 TEM image of HZSM-5 (a) and Zn/HZSM-5 (b and c) with EDX spectrum. The darker particles in (b) and (c) were the dispersed ZnO particles confirmed by EDX (d).

products were analysed using an online gas chromatograph (Agilent 7890B) equipped with a Plot-Q capillary column connected to a flame ionization detector(FID) to detect the hydrocarbons of methane, ethane, ethylene, C_3, benzene and toluene, and an HP-5 capillary column connected to another FID to detect the aromatics such as BTX, naphthalene, methylnaphthalene and C_{11+} aromatics, and a TDX-1 packed column connected to a thermal conductivity detector(TCD) to detect Ar, CO, CH_4 and CO_2.

3. Results and discussion

3.1 Catalyst characterization

X-ray diffraction (XRD) patterns (Fig. S1†) show that both catalysts have the typical diffraction peaks of MFI zeolite, and the characteristic peaks of ZnO at 31.8° and 36.3° are not found in zeolites with ZnO,[30,31] indicating that the Zn species on the ZSM-5 zeolite are highly dispersed after introducing zinc by impregnation. SEM images of HZSM-5 (Fig. S2†) show that this ZSM-5 zeolite has a well-defined hexagonal sheet crystal morphology with a mean thickness of 200–400 nm and a width of about 2–4 μm. The TEM images in Fig. 1 show that the nanocrystals of the zinc species are clearly formed (2–5 nm range) in the zeolite and the results of EDX proved the existence of zinc. Also, a small amount of zinc must enter the zeolite framework of ZSM-5 after calcination.

The BET surface area and micropore volume of both samples are listed in Table 1, which were determined by the standard BET equation and *t*-plot method, respectively. The surface areas of HZSM-5 and Zn/HZSM-5 were 339 and 269 $m^2\ g^{-1}$, respectively, whereas the corresponding pore volumes were 0.18 and 0.15 $cm^3\ g^{-1}$. Compared with the BET surface areas of HZSM-5, the surface area of Zn/HZSM-5 is reduced considerably after addition of zinc. Reduction of the surface area of the samples is probably ascribed to the pore filling and blocking of the mesopores during the impregnation presses.

3.2 Catalytic activity

CO promotion effectiveness on methane conversion. Studies on the catalytic performances of Zn/HZSM-5 in methane conversion with CO were first conducted at 773 K, 2.0 MPa, a space velocity of 4500 ml $g_{cat}^{-1}\ h^{-1}$ and $CO:CH_4 = 1:1$, and the results are shown in Fig. 2. It was found that the presence of CO can be efficiently activated and converted methane into hydrocarbons over Zn/HZSM-5 catalysts. The main products are 37.7% C_2 hydrocarbons (mainly ethane), 22.6% BTX (benzene, toluene and xylene), 29.0% naphthalenes (naphthalene and methylnaphthalene) and 10.1% C_{11+} aromatics at a methane conversion of about 1.8% with $CO:CH_4 = 1:1$. Moreover, supported Zn zeolite catalysts, such as Zn/Beta, Zn/MCM-22, Zn/ZSM-35, and Zn/MOR, were employed as catalysts for methane conversion with CO, and Zn/HZSM-5 catalyst exhibits the excellent catalytic performance (Fig. S4†). Also, 6% Zn/HZSM-5 has the highest activity among all HZSM-5-supported catalysts with different Zn contents (Fig. S5†).

To verify the role of CO in the methane conversion reaction, an experiment with helium instead of CO ($CO:CH_4 = 0:1$) was conducted under the same conditions. The results show that there was essentially no hydrocarbon to be detected in the test with Zn/HZSM-5 catalyst, and a small amount of CO_2 in the products is believed to be yielded *via* the CO disproportionation reaction ($2CO \rightarrow CO_2 + C$) on the tube wall of the reactor. As expected, an increase in the CO/CH_4 molar ratio from 1:1 to 8:1 is beneficial for methane conversion and a notable promotion effect of CO on the CH_4 conversion can be observed over Zn/HZSM-5 catalysts under the mild reaction conditions. The corresponding selectivity to naphthalenes increases from 29% to 60.5%, whereas the other products, such as BTX, C_{11+} aromatics and C_2–C_3 hydrocarbons, decrease. Apparently, the presence of CO in the reaction is beneficial for the methane conversion and the higher CO/CH_4 ratios favor the yield of naphthalene.

Table 1 Textural properties of HZSM-5 and Zn/HZSM-5

Sample	SiO_2/Al_2O_3	Content of Zn	Surface area($m^2\ g^{-1}$)			Pore volume ($cm^3\ g^{-1}$)	
			S_{BET} [a]	S_{Micro} [b]	S_{Ex} [c]	V_{total}	V_{Micro} [d]
HZSM-5	40	—	339.48	233.93	105.55	0.18	0.11
Zn/HZSM-5	40	5.93	269.16	197.13	72.03	0.15	0.10

SiO_2/Al_2O_3 and the loading content of zinc were determined by XRF. [a] BET surface area. [b] *t*-Plot micropore surface area. [c] *t*-Plot external surface area. [d] *t*-Plot micropore.

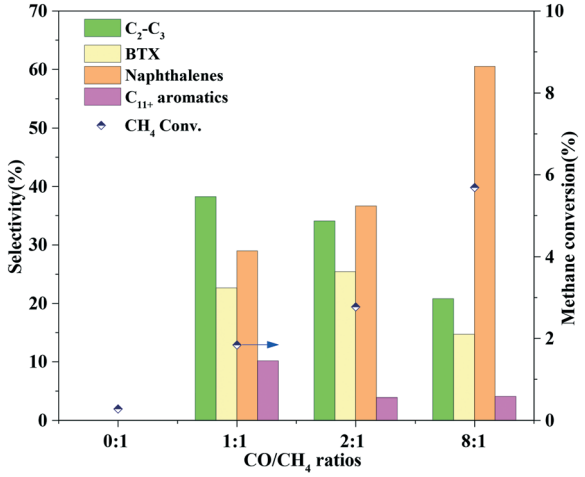

Fig. 2 The hydrocarbon selectivity and methane conversion. Reaction conditions: temperature = 773 K; pressure = 2.0 MPa; space velocity = 4500 mL g_{cat}^{-1} h^{-1}; He : CH_4 : Ar = 8 : 1 : 1, He : CO : CH_4 : Ar = 7 : 1 : 1 : 1, He : CO : CH_4 : Ar = 6 : 2 : 1 : 1, CO : CH_4 : Ar = 8 : 1 : 1; time on stream = 30 min.

Due to the highly inert properties of methane,[6] the higher reaction temperatures must favor higher conversion of methane. The effect of reaction temperature on the conversion of methane and product distribution was investigated over the Zn/HZSM-5 catalyst and the results are demonstrated in Fig. 3a. As expected, coupling reaction of methane with CO is quite sensitive to the reaction temperature in the range of 673 to 823 K, which is much lower than the traditional reaction temperature under CO-free conditions (up to 1300 K). With an increase in the temperatures from 773 to 823 K, the methane conversion rose from 5.9 to 9.1% and naphthalenes (naphthalene and methylnaphthalene, 73.2%) become dominant in the product distribution. On the other hand, a decrease in the reaction temperature to 673 K results in an unprecedented result that the selectivity to ethane alone reaches as high as 92% at 673 K at the methane conversion of 1.4%, without any naphthalene and methylnaphthalene formed at the initial stage of the reaction. Such a high selectivity to ethane has never been reported before in methane conversion. Apparently, the trend of ethane selectivity with reaction temperature is opposite from that of aromatics, indicating that C_2 hydrocarbons (ethane and a small amount of ethylene) are critical intermediates during the conversion of methane with CO over Zn/HZSM-5. Generally, the formation of ethane is yielded from the hydrogenation of ethylene by hydrogen atom transfer. In order to check the validity of this hypothesis, an experiment at the same temperature but higher pressure (5.0 MPa) was conducted, and the results are shown in Fig. 3c. It is found that more ethane is yielded with the decrease in the content of aromatics. Furthermore, the effect of reaction pressures on the ratio of ethylene/ethane in the products has been observed and the results are shown in Fig. S8.† It is obvious that the ratios of ethylene/ethane decrease with increasing reaction pressure. Therefore, ethane is the product of ethylene *via* hydrogenation.

The conversion of methane with CO is a volume reduction reaction and thus reaction pressure is another important parameter. As expected, higher reaction pressure is beneficial to the transformation of methane into hydrocarbons with carbon monoxide, as shown in Fig. 3b. Methane conversion is enhanced from 1.6% to 8.0% with an increasing reaction pressure from 0.1 to 4.0 MPa at 773 K. The corresponding selectivity to naphthalene and methylnaphthalene rises sharply from 33.6% to 51.4% with BTX selectivity obviously decreasing from 46% to 23.6%, which may indicate that the formation of polycyclic aromatics such as naphthalene comes from the further reaction of single ring aromatics.

Identification of carbon monoxide's role in the methane conversion. According to all the findings above, we can draw a preliminary conclusion that carbon monoxide is definitely involved in the process of methane transformation and contributes to the methane conversion at relatively low reaction temperature for the formation of the hydrocarbons. Isotope experiment is an effective approach to confirm whether the reactant participates in the reaction. In order to illustrate the

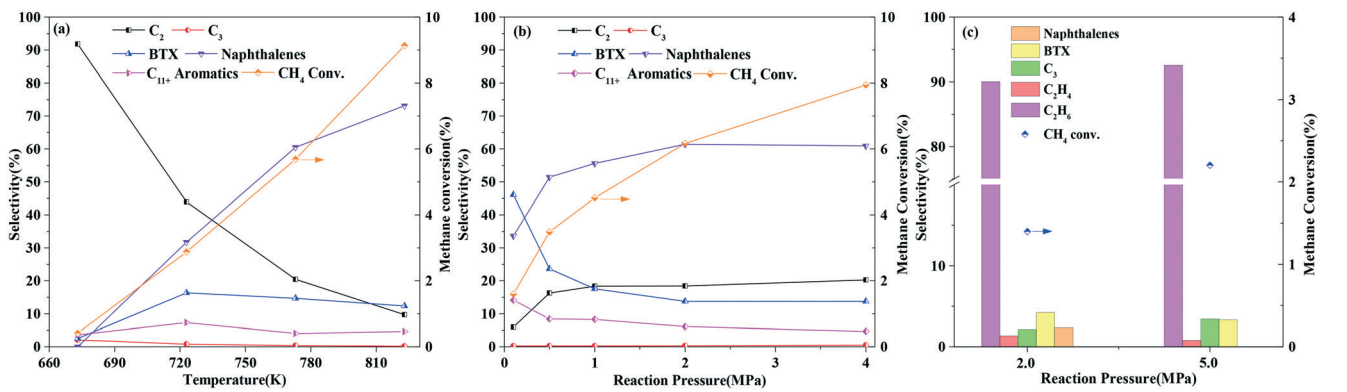

Fig. 3 The hydrocarbon selectivity and methane conversion. Reaction conditions: (a) space velocity = 4500 mL g_{cat}^{-1} h^{-1}, $CO/CH_4/Ar$ = 8 : 1 : 1, pressure = 2.0 MPa, temperature = 673 K, 723 K, 773 K and 823 K, time on stream = 30 min; (b) space velocity = 4500 mL g_{cat}^{-1} h^{-1}, $CO/CH_4/Ar$ = 8 : 1 : 1, pressure = 0.1, 0.5, 1.0, 2.0 and 4.0 MPa, temperature = 773 K, time on stream = 30 min; (c) space velocity = 2250 mL g_{cat}^{-1} h^{-1}, $CO/CH_4/Ar$ = 8 : 1 : 1, pressure = 2.0 and 5.0 MPa, temperature = 673 K, time on stream = 60 min.

CO evaluation pathway in the conversion of methane, isotope-trace experiments with ^{13}C labelled CO were conducted to explore the mechanism of methane transformation, and the results of ^{13}C distribution in the representative products are shown in Fig. 4. Apparently, all the products, such as ethane, benzene and naphthalene, contain ^{13}C atoms originated from ^{13}C labelled CO, indicating that CO really reacts with methane over the Zn/HZSM-5 catalysts under the present mild reaction conditions, which yields various hydrocarbon products. Remarkably, the ratio of ^{13}C to ^{12}C in all the hydrocarbon products is around 1 : 1 (Fig. 4b), which means that almost half of the total carbon atoms in all the products originated from methane, and the other half from CO. Based on these findings, we naturally deduce that the reaction between methane and CO yields crucial intermediate species bearing equimolar carbon atoms from methane and CO, followed by their transformations into various hydrocarbons on Zn/HZSM-5 zeolites.

^{13}C CP/MAS NMR spectroscopy was employed to monitor the changes of the intermediate species captured on the surface of Zn/HZSM-5 with ^{13}C labelled carbon monoxide under the different reaction temperatures of 643, 673 and 723 K, and the results are shown in Fig. 6. It can be seen that there is a strong signal at δ = 173 ppm which represents the produced surface formate species, and another obvious signal at δ = 186 ppm (Fig. 5a), assigned to the carbonyl groups of acetyl compounds (such as acetic acid), is found at the lower reaction temperature of 643 K and 673 K, whereas the signal at δ = 21 ppm, corresponding to the ^{13}C labelled methyl groups of acetyl compounds/acetic acid, is not observed.[29,32,33] These findings clearly show that the intermediates were produced by the coupling of unlabelled methane and ^{13}C labelled CO under the present mild reaction conditions. With an increase in reaction temperatures, a new signal at δ = 132 ppm (Fig. 5c), which corresponds to aromatics,[16] appears with the disappearance of the signal at δ = 186 ppm (Fig. 5a). Among all the products in the present test, acetic acid was definitely detected by GC-MS, but it is possible that acetic acid is only the product of the acetyl compound, not the key intermediate of methane conversion with CO. Anyhow, these results suggest that the further transformation of acetyl compounds (or acetic acid) results in the formation of aromatics at a relatively higher reaction temperature of 643 K. Also, the results of the ^{13}C CP/MAS NMR spectra indicate that the formation of the initial C–C bond occurs *via* carbonylation of methane with CO to acetyl compounds/acetic acid, where the carbon atom of the methyl groups comes from methane and the carbonyl groups comes from CO, followed by further transformation into higher molecular weight hydrocarbons and aromatics.

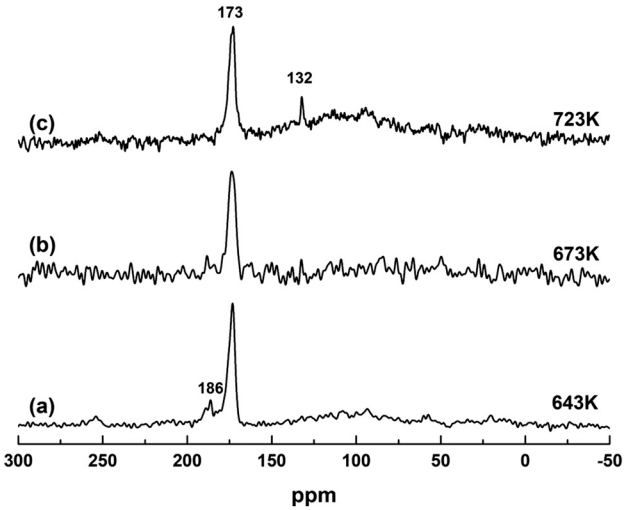

Fig. 5 ^{13}C CP/MAS NMR spectra of the products after co-reaction of carbon monoxide and methane in a continuous flow for 10 min. 0.1 g Zn/H-ZSM-5; He/CO/CH_4 = 8 : 8 : 1; pressure = 1.0 MPa, space velocity = 3000 mL g_{cat}^{-1} h^{-1} (a)–(c) ^{13}CO and CH_4 at 643 K, 673 K and 723 K. Spinning rate = 12 kHz.

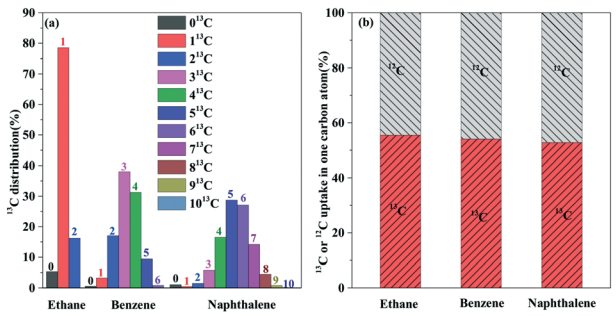

Fig. 4 The isotope results of ethane, benzene, and naphthalene collected after the reaction of ^{13}CO and CH_4 analysed by GC-MS. Reaction conditions: temperature = 773 K, pressure = 1.0 MPa, space velocity = 3000 mL g_{cat}^{-1} h^{-1}, CO/CH_4/Ar = 8 : 1 : 1, reaction time = 60 min.

Pathway for aromatic formation *via* the intermediate of acetic acid from CH_4 and CO. According to all the findings above, acetyl compound/acetic acid is the intermediate for the formation of aromatics and other hydrocarbons based on the ^{13}C NMR results. In order to further verify this contention, some simulation tests with possible intermediates and CO as reactants were conducted on Zn/HZSM-5 and the results are shown in Fig. 6. In the test with acetic acid + CO, C_2–C_3 hydrocarbons, BTX, naphthalene and methyl naphthalene were actually observed, but detailed product distribution is different from the one obtained in the test with methane + CO. This indicates that direct conversion of acetic acid to aromatics might be infeasible under the present conditions. It is well known that at high temperatures, acetic acid can easily produce ketene,[34,35] which is believed to be the key intermediate for ethylene production[36] in synthesis gas conversion. Also, in the above test, at the low temperature of 673 K, a large amount of ethane was detected and proved to be the product of ethylene by hydrogenation. Considering that Zn/HZSM-5 catalyst is one of the superior catalysts for ethylene aromatization to aromatics, the experiment with ethylene + CO as reactants was performed under the same conditions. Apparently, its product distribution is almost similar to that of the reaction with methane + CO (Fig. 6).

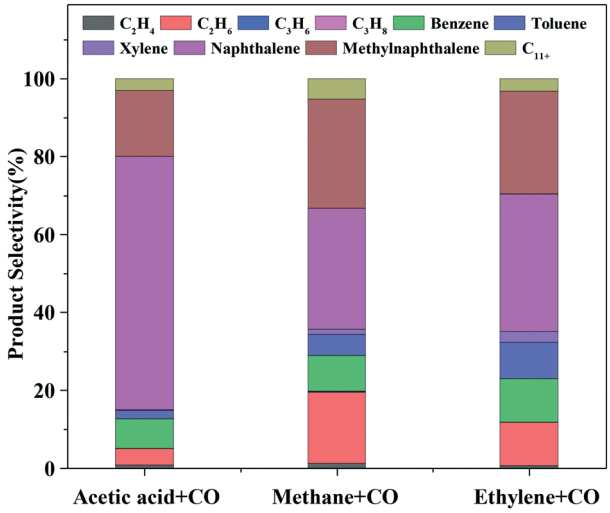

Fig. 6 The hydrocarbon distribution of the reaction of acetic acid + CO, ethylene + CO, and methane + CO on Zn/H-ZSM-5. Reaction conditions: T = 773 K; P = 2.0 MPa; time on stream = 60 min. Acetic acid and CO experiment: 30 mL min^{-1} CO carried acetic acid into the reactor. Ethylene and CO experiment: 1% ethylene in feed gas, 19%N_2, 80%CO, CO/ethylene = 80 : 1 space velocity = 4500 mL g_{cat}^{-1} h^{-1}.

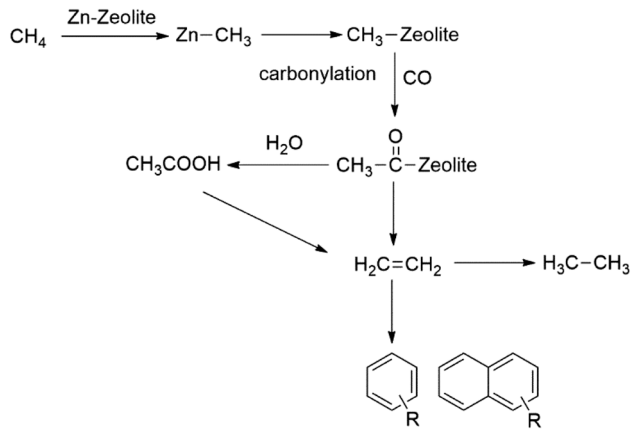

Fig. 7 Proposed reaction path of the co-reaction of methane and carbon monoxide on Zn/HZSM-5.

Based on these results, we proposed a possible pathway for the coupling conversion of methane with CO to aromatics by carbonylation (shown in Fig. 7). After activation by zinc, CH_4 is first converted into a methyl compound and then transfers to zeolite, where carbonylation reaction occurs. The produced acetyl compound and/or acetic acid dehydrated to ketene, an intermediate for the formation of ethylene. The conversion of ethylene to aromatics occurs readily on the ZSM-5 zeolite and thus a large amount of aromatics is produced. Ethane is yielded through the hydrogenation of ethylene by hydrogen transfer reaction on the surface of zeolite catalysts. In addition, the water, produced from the dehydration reaction of acetic acid, could yield some CO_2 through the water–gas shift reaction and provide hydrogen. Also, the pathway for constructing the first C–C bond to hydrocarbons by methane carbonylation is proposed.

4. Conclusions

In summary, coupling conversion of methane with CO was conducted under mild conditions (<773 K). Methane conversion can be promoted by the incorporation of carbon monoxide over Zn/HZSM-5 catalysts. At high temperature (823 K), selectivity to aromatics alone reaches 80%, whereas at low temperature (673 K), ethane selectivity of 92% was obtained, which is formed by the hydrogenation of ethylene. The isotope tracer investigations reveal that the underlying mechanism is related to the equimolar cross-coupling of CH_4 with CO *via* a carbonylation pathway. The intermediate chain of acetyl compound/acetic acid–ethylene can be confirmed by ^{13}C CP/MAS NMR and the designed comparative experiments. The aforementioned mechanistic understandings lay down the scientific foundations for the further design of superior catalysts for methane conversion.

Conflicts of interest

There are no conflicts to declare.

Acknowledgements

We acknowledge the financial support from the National Natural Science Foundation of China (Grant No. 21972141, No.21991094, and No.21991090), and the "Transformational Technologies for Clean Energy and Demonstration", Strategic Priority Research Program of the Chinese Academy of Sciences (Grant No. XDA21030100). The authors are grateful to Prof. ShengJun Huang for fruitful discussions. We acknowledge Mrs. Yanli He and Mr. Yijun Zheng for their help in the characterization of the catalysts.

References

1 Y. Li and G. Veser, *Energy Technol.*, 2020, **8**, 2000460.
2 P. He, R. Gatip, M. Yung, H. B. Zeng and H. Song, *Appl. Catal., B*, 2017, **211**, 275–288.
3 P. Tang, Q. Zhu, Z. Wu and D. Ma, *Energy Environ. Sci.*, 2014, **7**, 2580–2591.
4 P. Schwach, X. Pan and X. Bao, *Chem. Rev.*, 2017, **117**, 8497–8520.
5 X. G. Guo, G. Z. Fang, G. Li, H. Ma, H. J. Fan, L. Yu, C. Ma, X. Wu, D. H. Deng, M. M. Wei, D. L. Tan, R. Si, S. Zhang, J. Q. Li, L. T. Sun, Z. C. Tang, X. L. Pan and X. H. Bao, *Science*, 2014, **344**, 616–619.
6 F. Larkins and A. Khan, *Aust. J. Chem.*, 1989, **42**, 1655–1670.
7 A. Holmen, O. Olsvik and O. A. Rokstad, *Fuel Process. Technol.*, 1995, **42**, 249–267.
8 J. J. Shan, M. W. Li, L. F. Allard, S. S. Lee and M. Flytzani-Stephanopoulos, *Nature*, 2017, **551**, 605–608.
9 M. H. Mahyuddin, Y. Shiota and K. Yoshizawa, *Catal. Sci. Technol.*, 2019, **9**, 1744–1768.

10 N. Agarwal, S. J. Freakley, R. U. McVicker, S. M. Althahban, N. Dimitratos, Q. He, D. J. Morgan, R. L. Jenkins, D. J. Willock, S. H. Taylor, C. J. Kiely and G. J. Hutchings, *Science*, 2017, **358**, 223–226.
11 J. Bedard, D. Y. Hong and A. Bhan, *Phys. Chem. Chem. Phys.*, 2013, **15**, 12173–12179.
12 V. R. Choudhary, K. C. Mondal and S. A. R. Mulla, *Angew. Chem., Int. Ed.*, 2005, **44**, 4381–4385.
13 V. R. Choudhary, A. K. Kinage and T. V. Choudhary, *Science*, 1997, **275**, 1286–1288.
14 T. Baba and Y. Abe, *Appl. Catal., A*, 2003, **250**, 265–270.
15 O. A. Anunziata, G. V. G. Mercado and L. B. Pierella, *Catal. Lett.*, 2003, **87**, 167–171.
16 M. V. Luzgin, V. A. Rogov, S. S. Arzumanov, A. V. Toktarev, A. G. Stepanov and V. N. Parmon, *Angew. Chem., Int. Ed.*, 2008, **47**, 4559–4562.
17 G. E. Keller and M. M. Bhasin, *J. Catal.*, 1982, **73**, 9–19.
18 S. Arndt, G. Laugel, S. Levchenko, R. Horn, M. Baerns, M. Scheffler, R. Schlogl and R. Schomacker, *Catal. Rev.: Sci. Eng.*, 2011, **53**, 424–514.
19 U. Zavyalova, M. Holena, R. Schlogl and M. Baerns, *ChemCatChem*, 2011, **3**, 1935–1947.
20 M. Lin and A. Sen, *Nature*, 1994, **368**, 613–615.
21 G. V. Nizova, G. Suss-Fink, S. Stanislas and G. B. Shul'pin, *Chem. Commun.*, 1998, 1885–1886.
22 Y. Taniguchi, T. Hayashida, H. Shibasaki, D. G. Piao, T. Kitamura, T. Yamaji and Y. Fujiwara, *Org. Lett.*, 1999, **1**, 557–559.
23 M. Asadullah, T. Kitamura and Y. Fujiwara, *Angew. Chem., Int. Ed.*, 2000, **39**, 2475–2478.
24 R. A. Periana, O. Mironov, D. Taube, G. Bhalla and C. J. Jones, *Science*, 2003, **301**, 814–818.
25 S. Naito, T. Karaki and T. Iritani, *Chem. Lett.*, 1997, 877–878, DOI: 10.1246/cl.1997.877.
26 H. Wang, Z. M. Liu, J. H. Shen, H. C. Liu and J. L. Zhang, *Catal. Commun.*, 2005, **6**, 343–346.
27 S. T. Liu, L. S. Wang, Q. Dong, R. Ohnishi and M. Ichikawa, in *Natural Gas Conversion V*, ed. A. Parmaliana, D. Sanfilippo, F. Frusteri, A. Vaccari and F. Arena, Elsevier Science Publ B V, Amsterdam, 1998, vol. 119, pp. 241–246.
28 R. Ohnishi, S. T. Liu, Q. Dong, L. Wang and M. Ichikawa, *J. Catal.*, 1999, **182**, 92–103.
29 X. M. Wang, G. D. Qi, J. Xu, B. J. Li, C. Wang and F. Deng, *Angew. Chem., Int. Ed.*, 2012, **51**, 3850–3853.
30 Z. R. R. Tian, J. A. Voigt, J. Liu, B. McKenzie, M. J. McDermott, M. A. Rodriguez, H. Konishi and H. F. Xu, *Nat. Mater.*, 2003, **2**, 821–826.
31 M. G. Ruiz, D. A. S. Casados, J. A. Pliego, C. M. Alvarez, E. S. de Andres, D. S. Tartalo, R. S. Vaque and M. G. Casas, *React. Kinet., Mech. Catal.*, 2020, **129**, 471–490.
32 J. F. Wu, W. D. Wang, J. Xu, F. Deng and W. Wang, *Chem. – Eur. J.*, 2010, **16**, 14016–14025.
33 M. V. Luzgin, V. A. Rogov, N. S. Kotsarenko, V. P. Shmachkova and A. G. Stepanov, *J. Phys. Chem. C*, 2007, **111**, 10624–10629.
34 J. Stubenrauch, E. Brosha and J. M. Vohs, *Catal. Today*, 1996, **28**, 431–441.
35 Y. F. Zhang, D. R. Mullins and A. Savara, *J. Phys. Chem. C*, 2019, **123**, 4148–4157.
36 F. Jiao, X. L. Pan, K. Gong, Y. X. Chen, G. Li and X. H. Bao, *Angew. Chem., Int. Ed.*, 2018, **57**, 4692–4696.

